Low Resonant Frequency Beam Design for a Piezoelectric Energy Harvesting Device

by

John A. Brewer

Submitted to the Department of Mechanical Engineering
in partial fulfillment of the requirements for the degree of

Bachelor of Science in Mechanical Engineering

at the

MASSACHUSETTS INSTITUTE OF TECHNOLOGY

May 2005 [June 2005]

Author .....
Department of Mechanical Engineering
May 6, 2005

Certified by .....
Sang-Gook Kim
Associate Professor of Mechanical Engineering
Thesis Supervisor

Accepted by .....
Ernest G. Cravalho
Chairman, Undergraduate Thesis Committee

Low Resonant Frequency Beam Design for a Piezoelectric Energy Harvesting Device

by

John A. Brewer

Submitted to the Department of Mechanical Engineering
on May 6, 2005, in partial fulfillment of the
requirements for the degree of
Bachelor of Science in Mechanical Engineering

Abstract

The TREAD Act of 2000 proposed rules that will soon make tire pressure sensors standard on all automobiles. The trend seems to be for small chips that can be imbedded in tires and perform sensing, signal processing, and RF transmission in one package. But powering these devices will be another challenge that must be addressed.

This project deals with powering these sensors by harvesting environmental vibrational energy and eliminating the need for batteries. Using MEMS technology, a thin film Piezoelectric Micropower Generator device could be constructed. The PMPG is simply a cantilever structure tuned to resonate at environmental frequencies. At resonance, sizable strain is induced in a layer of the beam made from the piezoelectric material, PZT, thereby generating electricity.

Recent studies have found that the most available environmental frequencies are on the order of 100 Hz. Current PMPG structures were designed to operate at 20 kHz. This project is aimed at understanding how to design low resonance beams while keeping them compact. Large one-dimensional cantilevers of low resonant frequency would pose serious packaging problems for the device.

Two-dimensional spiral beams were designed and analyzed using analytical as well as finite element methods. The dependence on length was found to be a function of $l^{-1.3}$ rather than l^{-2} of conventional one-dimensional beams. A variety of designs were developed using ANSYS which have resonant frequencies in the target range. The mode shapes were also simulated. To compare analysis with experiments, simple mock-up designs are planned to be fabricated from the polymer SU-8.

Thesis Supervisor: Sang-Gook Kim
Title: Associate Professor of Mechanical Engineering

Acknowledgments

Thanks to Professor Sang-Gook Kim for allowing me to complete my undergraduate thesis under his supervision. Thanks to Wonjae Choi for his help on nearly every aspect of this thesis. His assistance was invaluable and always gracious. The author sincerely hopes that he will have great success as he continues his research on energy harvesting. Thanks also to Soohyung Kim who provided a tremendous amount of assistance with ANSYS and the understanding of finite element analysis.

Contents

List of Figures

1 Introduction

In the wake of several automobile fatalities dealing with roll-over of Ford Explorers due to under inflated Firestone tires, Congress passed the Transportation Recall Enhancement, Accountability, and Documentation Act. One of the rules proposed in the TREAD Act was a call for vehicles under ten thousand pounds to have required tire pressure monitoring systems. These monitoring systems could deliver valuable information to the driver to prevent accidents like those in the Firestone tragedies.

Ideas for implementing these monitoring systems vary, but many are convinced that a "one chip" solution is the most efficient and cost-effective [1]. A single chip that could be planted in the tires of vehicles and sense pressure, process the signals, and then transmit the information back to a central computer is the goal of these advocates. Producing a single chip and implanting it into tires would present another high-volume application for the rapidly expanding field of microelectromechanical systems (MEMS). These microscopic systems, constructed through batch microfabrication technologies, give engineers more power at the small scale than ever before. The ability to design and fabricate such small devices at low cost allows for a variety of potential applications that will permeate not only the auto industry, but every other facet of engineering as well.

Pressure sensors, of course, need power to operate, and therein lies the problem that this project is aimed at solving. Currently, batteries have been the only solution to powering these devices. But the call from auto makers for a ten year service life presents a great challenge for battery manufacturers. A better solution may be to eliminate the battery entirely and add another function to the "one chip" design. This added function would be autonomous power generation.

At the micro scale, renewable energy harvesting from the environment seems a particularly attractive method. If power can be generated at a sufficient level to eliminate the need for batteries, these pressure sensors will then have infinite life and the capacity to be set in place and monitored continuously without the need for significant maintenance. Energy sources already suggested include solar power,

electromagnetic fields, thermal gradients, and fluid flow. The energy source most accessible for MEMS sensors, however, is mechanical vibration, scavenged from the surrounding environment.

Possible tools for capturing mechanical vibration are piezoelectric materials, which create electric charge when subjected to mechanical strain. Mechanical energy is converted to electric energy efficiently, without the need for added power. Clearly, this is an attractive method for powering wireless sensors.

The focus of this project involves the Piezoelectric Micro Power Generator (PMPG) for powering wireless sensors. The PMPG represents the first thin-film, MEMS scale, piezoelectric generator. The PMPG device utilizes the piezoelectric material, lead zirconate titanate (PZT), in its d_{33} mode [2]. The basic device consists of a cantilevered beam with a PZT layer and an interdigitated electrode on top of the PZT layer. By designing the beams to resonate at the frequency of the ambient vibration, sizable strain will be induced in the PZT layer of the beam and then electricity is generated. The charge produced is rectified and stored in a capacitor.

The challenges that will be addressed in this project deal with the design of the beam's natural frequency. Previous work on the beam design was with the intent of producing beams with a natural frequency of 20 kHz. This calls for simple rectangular beam structures of small length. Recent research, however, has made it clear that "low level vibrations occurring on many household appliances and everyday objects in and around buildings appear to have a fundamental mode on the order of 100 Hz" [3].

This vastly new target for resonant frequency of the beam presents design challenges. Low natural frequencies near 100 Hz for beam structures require a simple rectangular cantilevered beam to be much longer than one with a resonant frequency of 20 kHz. Increasing both the width and length of the beams to meet the new target frequency forces the devices to become larger, which makes packaging difficult. The goal of this project is to develop options for beam design that minimize the required space for the beam while achieving resonance in the 100-200 Hz range.

2 Device Description

PMPG beam fabrication is an already established process [4] designed to require only three photo masks. The beam consists of three layers along with an interdigitated electrode and a proof mass if one is so desired.

2.1 Beam Fabrication

The layered structure of the PMPG is shown in Figure 1. The first layer, the main structure of the beam, is a membrane deposited onto a (100) Silicon wafer. This membrane layer is 0.4 μm thick SiNx, which has a high Young's modulus and yield strength. Those properties, along with added membrane layers of PECVD oxide and thermal oxide serve to counteract the residual stress of the composite beam and prevent warpage upon release. These additional layers add approximately 0.4 μm in thickness.

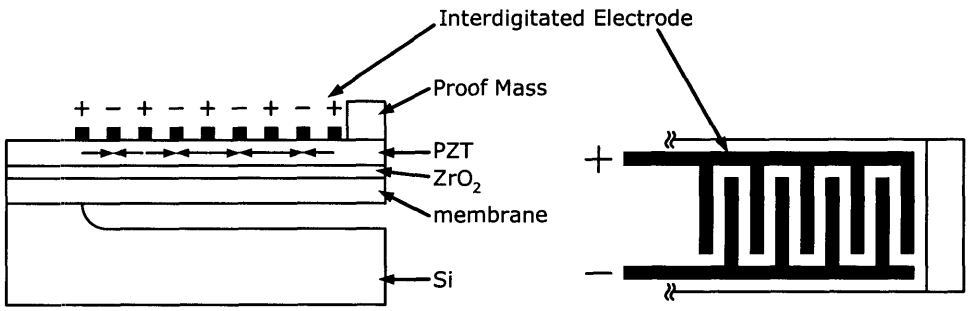

Figure 1: PMPG beam layer schematic [2].

The second layer is 50 nm thick ZrO_2. It is deposited by sol-gel spin-on process over the membrane before being dried and annealed. The ZrO_2 serves as a diffusion barrier layer to prevent electrical charge from escaping the piezoelectric layer. The PZT ($Pb(Zr,Ti)O_3$) layer is spun on the substrate in four cycles to achieve a thickness of 0.48 μm and then annealed. The PZT and membrane layers are patterned via RIE with BCl_3:Cl_2 (30:10) on the first mask.

The interdigitated electrode consists of 20 nm Ti and 200 nm Pt, deposited by e-beam evaporation. The electrode is patterned by a lift-off procedure on the second mask. Finally, SU-8 is spin-coated and patterned with the third mask to create a proof mass. This added polymer at the tip of the beam allows for fine tuning of the natural frequency.

Isotropic XeF_2 vapor etching is used to release the beam from the Silicon substrate. Typical KOH etching attacks PZT and is unsuitable to release the structure. Instead, the XeF_2 vapor uses the PZT as a mask and performs the release quite well. A picture of a completed PMPG structure is shown in Figure 2.

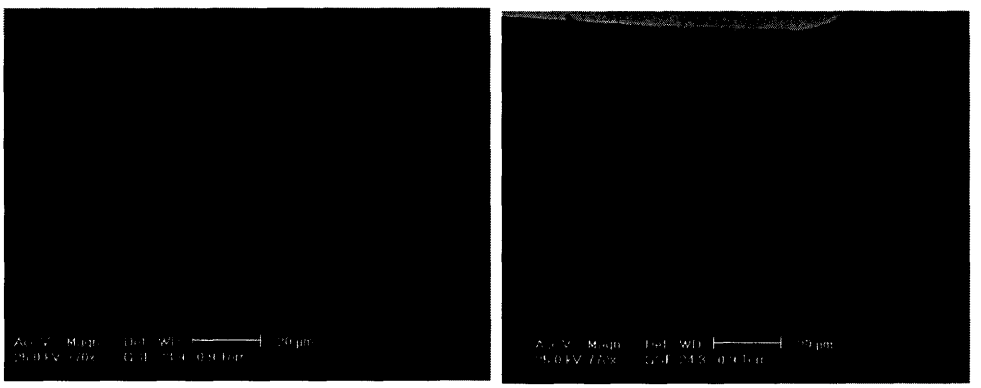

Figure 2: Scanning electron microscope images of the current PMPG beam design. [2]

2.2 Circuitry

Along with fabrication of the beam itself, added circuitry is necessary for harvesting energy. Vibrating at the beam's resonant frequency causes the PZT layer to undergo mechanical stress and strain that oscillate between tension and compression. The oscillation produces an alternating current and requires a rectifying circuit and storage capacitor to extract DC power from each beam. A complete generating device may actually consist of a cluster of beams and rectifying circuits in order to generate substantive power.

3 Analytical Estimates and Theory

Traditional beam theory serves to give a theoretical foundation to the exploration of resonant frequencies in more complex beam structures. By understanding how a simple one-dimensional cantilevered beam vibrates, perhaps comparisons can be made with many other configurations.

3.1 Static Deflection of a Cantilever Beam

For small deflections, a beam remains within its elastic region. For a beam of uniform cross-section, the beam curvature, κ, is the second derivative of the beam deflection curve:

$$\kappa = \frac{\partial^2 y}{\partial x^2} = \frac{M}{EI}, \tag{1}$$

equal to the ratio of bending moment, M and flexural rigidity, EI. E represents the Young's modulus of the beam material and I, the cross-sectional moment of inertia. The bending moment is then related to shear force, V, and lateral load, q:

$$M = EI\frac{\partial^2 y}{\partial x^2}, V = EI\frac{\partial^3 y}{\partial x^3}, q = -\frac{\partial^4 y}{\partial x^4}. \tag{2}$$

For a cantilevered beam, with end load P and length L, the bending moment is:

$$M(x) = -PL\left(1 - \frac{x}{L}\right). \tag{3}$$

Integrating twice to find the deflection curve yields:

$$\frac{\partial y}{\partial x} = \frac{1}{EI}\int_0^x M(x)\,dx = \frac{PL}{EI}\left(x - \frac{x^2}{2L}\right), \tag{4}$$

$$y(x) = \frac{1}{EI}\int_0^x \frac{\partial y}{\partial x}\,dx = \frac{PL}{EI}\left(\frac{x^2}{2} - \frac{x^3}{6L}\right). \tag{5}$$

Thus the maximum displacement is given by:

$$y(L) = -\frac{PL^3}{3EI}. \tag{6}$$

3.2 Rayleigh Energy Method

Rayleigh's energy methods can be used to determine the lowest natural frequency of continuous systems like beams [5]. Assuming a mass m vibrates without damping, the total energy of the systems remains constant:

$$\frac{d}{dt}(T+V)=0, \tag{7}$$

where $T = 1/2mv^2$ is kinetic energy of the mass and $V = 1/2kx^2$ is the elastic energy. Assuming simple harmonic motion, $x = x_0 cos(\omega t)$:

$$T_{\max}=\frac{1}{2}mx_0^2w^2 \text{ and } V_{\max}=\frac{1}{2}kx_0^2. \tag{8}$$

Setting T_{max} and V_{max} equal yields a familiar result for natural frequency,

$$\omega=\sqrt{\frac{k}{m}}. \tag{9}$$

These methods are easily extended to cantilevered beams. Expressions for T_{max} and V_{max} are found by integrating over the length of the beam:

$$T_{\max}=\frac{1}{2}\int \dot{y}^2\,dm=\frac{1}{2}\omega^2\int y^2\,dm, \tag{10}$$

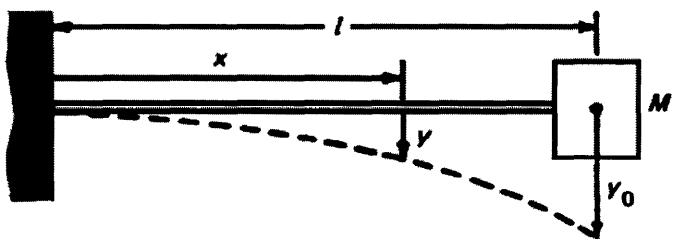

Figure 3: A beam of length l, proof mass M, and deflection curve, y [5].

where m is mass per unit length, y is the assumed amplitude of deflection, and ω is the natural frequency. With bending moment M imposed on the beam and θ, the slope of the elastic curve:

$$V_{\max} = \frac{1}{2}\int M\, d\theta = \frac{1}{2}\int \frac{M}{R}\, dx = \frac{1}{2}\int EI\left(\frac{d^2y}{dx^2}\right)^2 dx, \tag{11}$$

where R is the radius of curvature and EI is the flexural rigidity. These relationships hold only for small enough deflection such that: $\theta = dy/dx$ and $Rd\theta = dx$ remain true. Setting T_{max} and V_{max} equal yields an expression for natural frequency:

$$\omega^2 = \frac{\int EI\left(\frac{d^2y}{dx^2}\right)^2 dx}{\int y^2\, dm}. \tag{12}$$

This frequency represents the lowest natural frequency of transverse vibration. The static deflected shape is assumed and appropriate boundary conditions are applied. As seen in Figure 3 [5], the PMPG can be represented by a cantilevered beam, with a proof mass on its free end. From Equation (5), substituting $P = Mg$ for the proof mass, the static deflection curve is $y = y_0/(2l^3)(3lx^2 - x^3)$, where y_0 is the maximum deflection from Equation (6). Using the expression for V_{max} and T_{max} obtained above:

$$\int_0^l EI\left(\frac{d^2y}{dx^2}\right)^2 dx = EI\int_0^l \left(\frac{y_0}{2l^3}\right)^2 (6l - 6x)^2\, dx = \frac{3EI}{l^3}y_0^2 \tag{13}$$

$$\int y^2\, dm = \int_0^l y^2 \frac{m}{l}\, dx + y_0^2 M = y_0^2\left(M + \frac{33}{140}m\right). \tag{14}$$

Dividing the expressions eliminates maximum deflection y_0 from the equation, leaving natural frequency in terms of geometric constants and material properties:

$$\omega^2 = \frac{3EI}{\left(M + \frac{33}{140}m\right)l^3}\ (\text{rad/s})^2. \tag{15}$$

3.3 Size and Frequency of Current and Future Structures

The relationship between resonant frequency and beam length is shown in Figure 4 over the desired range of frequencies for a 1.2 μm thick typical PMPG composite beam. Detailed analysis for composite beam structures will not be discussed in this thesis. It should be noted that flexural rigidity, EI, is evaluated as a function of each of the component materials. For a complete discussion, see Opila [6].

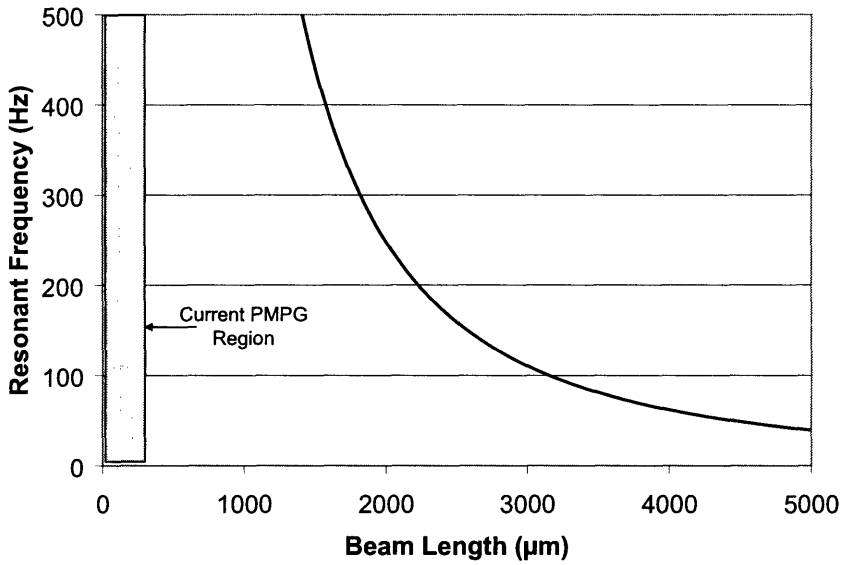

Figure 4: Relationship of resonant frequency and beam length. Theoretical data for a one-dimensional PMPG composite beam, 1.2μm thick.

It becomes clear from this relationship that achieving resonant frequencies near the target of 100 Hz requires a structure of considerable length. Current PMPG's have lengths and widths of not more than 200 μm. Extending a single cantilever to a length on the order of 2 mm is impractical. These conflicting functional requirements call for the length of the beam to be long enough to achieve low resonant frequencies, but without extending in only one direction. Instead, a more compactly shaped two-dimensional beam could be used. The idea of spreading the beam length over two dimensions leads naturally to designs that spiral inward, with any necessary proof mass added at the end of the beam and center of the structure.

4 Finite Element Analysis

Finite Element analysis is the next step in simulating a beam's resonant frequencies more precisely. The two-dimensional beam structures differ considerably from the simple one-dimensional beams, and finite element results serve to point out any problems of approximating with simple beam theory. FEA is used to quickly eliminate some designs and fix a range of experimental parameters for further analysis. The finite element analysis software ANSYS is used throughout the project. Analysis simulations are performed using the properties of materials planned for experimental use.

4.1 Choosing Shape

One of the first questions answered with ANSYS is the general design shape. After several analyses, it was becomes clear that extending the beam in arcs rather than rectangular shapes was better for the PMPG. It is noted that circular shapes have lower spring constants and consequently allow for more displacement from a given vibration amplitude. More displacement increases the strain levels of the structure and should in turn produce more power. The stress concentrations found in circular structures are also more uniform. No troubling stress concentrations are found in the circular structures, while a rectangular structure's sharp corners pose a greater threat.

4.2 Fixing Experimental Parameters of Size and Material

The materials that will be used in the PMPG have already been mentioned and thus choice of materials is not a factor in actual design of the device. However, for the analysis of this project the exact materials of the PMPG are not used in order to preserve cost. Composite beam analysis is also neglected because the exploration of shape and resonant frequency is the primary focus. Originally, the experimental designs were planned using Silicon on insulator (SOI) wafer. Availability, however, forced the polymer SU-8 to be used instead.

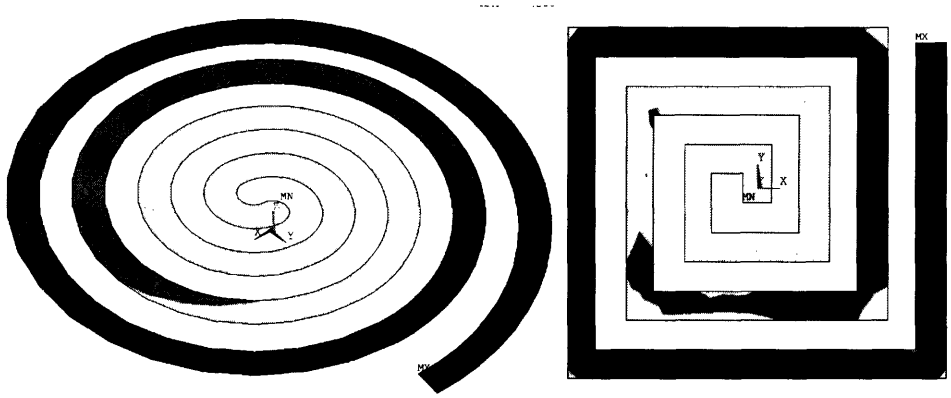

Figure 5: The Von Mises stress levels for circular and rectangular spiraled beams. Note the stress concentrations found in the rectangular beam.

4.2.1 Archimedes' Spiral

The exact design of the spiraled beam is represented by Archimedes' Spiral, given by the polar equation, $r = a\theta$, where a is a parameter which controls the gap between consecutive inner and outer arcs of the spiral. The arc length, s, is then:

$$s = \frac{1}{2}a\left[\theta\sqrt{\theta^2+1} + \ln\left(\theta + \sqrt{\theta^2+1}\right)\right], \tag{16}$$

For this design, the beam width and the gap between arcs of the spiral are equal. This sets the parameter, $a = \text{width}/(2\pi)$. The above formula is used here to solve for the equivalent beam length for spiral structures.

4.2.2 Simulated Beam Sizes

A beam width of 40 μm is considered the minimum to accommodate an interdigitated electrode with ease, and the expected thickness with all layers is 1.2 μm. To achieve frequencies on the order of 100 Hz with SU-8, thickness is increased to 25 μm, with widths of 150 μm, 200 μm, and 250 μm in various tests. True PMPG's of similar size are capable of being produced.

4.3 Modal Analysis

ANSYS calculates both resonant frequencies and their corresponding mode shapes. The high aspect ratio (width to thickness) of the structure makes the use of a shell element both necessary and applicable. The eight node structural shell, SHELL93 in ANSYS, is used throughout the project for all design variations. An example of the mesh is shown in Figure 6.

Figure 6: Typical FEA mesh of the spiral structure with a SHELL93 element.

Modal analysis in ANSYS provides information about free vibration only. Stiffness and mass effects are held constant and damping is ignored. No time varying forces, displacements, pressures, or other externalities are applied. Mode shapes are extracted using the Block-Lanczos method.

The ANSYS code used for modal analysis can be seen in Appendix A. The total lengths of the designed beams vary from 7.2 mm to 35.6 mm depending on width and number of turns in radians. The density of SU-8 is 2200 kg/m^3, with a Young's modulus of 4.02 GPa. The low Young's modulus of SU-8 is the main reason for the large increase in thickness from typical PMPG dimensions. In the ANSYS code, the unit of length was scaled to millimeters to accommodate imported Solidworks documents. The results are presented in the true dimensions of the PMPG: micrometers.

4.3.1 Modal Analysis Results: Resonant Frequencies

The resonant frequencies up to 700 Hz are calculated, with the lowest frequency plotted in Figure 7. The overall trends retain their shape from one-dimensional analysis, but there are several details that changed.

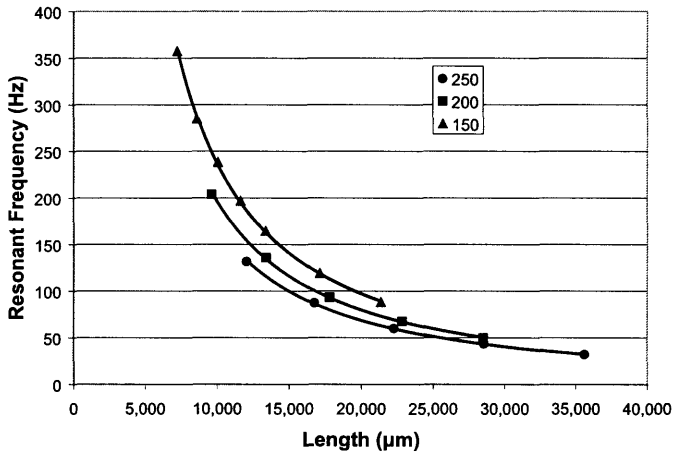

Figure 7: Resonant frequency vs. length for beam widths of 150, 200, and 250 μm. Frequency is no longer independent of width.

Resonant frequency for a spiral beam is not independent of width as is the case with a one-dimensional beam. Increases in width tend to shift the curve down in frequency, which is consistent with the intuition of the larger structure having a lower resonance. The other striking difference from the one-dimensional case is the overall dependence on length. Instead of varying with l^{-2}, resonant frequency varies with l^{-k}, where k is approximately 1.3 for the data collected.

The redirection of the beam length has a definite effect on the relationship between resonant frequency and length. This relationship can be more clearly seen in Figure 8. The Rayleigh estimates and ANSYS simulation results of resonant frequency do not directly correspond. In fact, the relationship between the two calculations is not linear, but rather another power function, with ANSYS frequencies varying as a function of the Rayleigh frequencies to approximately a power of 0.6.

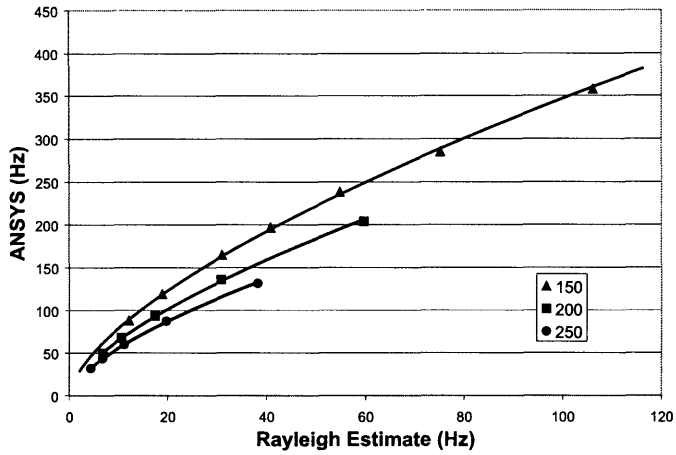

Figure 8: Comparison of ANSYS simulation results and Rayleigh frequency estimates.

One possible reason for the nonlinear relationship between ANSYS and Rayleigh estimates for one-dimensional beams is their difference of internal moments. A one-dimensional beam is subject to a pure bending moment, but two dimensional spiral beams have both a bending moment as well as a twisting moment or torsional component. This added moment complicates any attempts at analytical analysis significantly. Further examination of the internal moments of the spiral structures could yield deflection curves which would allow for an estimate of resonant frequency.

4.3.2 Modal Analysis Results: Mode Shapes

The first mode shape represents the primary deflection of the beam. Every part of the beam deflects to the same side of the horizontal plane. As a unit, the beam oscillates in the z direction. Renderings of the deformed shape are shown in Figure 9. The first or primary mode of resonance closely resembles deformation under the static load of its own weight. This primary mode is the most useful for power generation and must be maximized. It should be the resonance target of incoming environmental vibration.

The higher frequency modes exhibit not only an oscillation in the z direction, but also a more pronounced torque about the x and y axes. Figure 10 shows examples

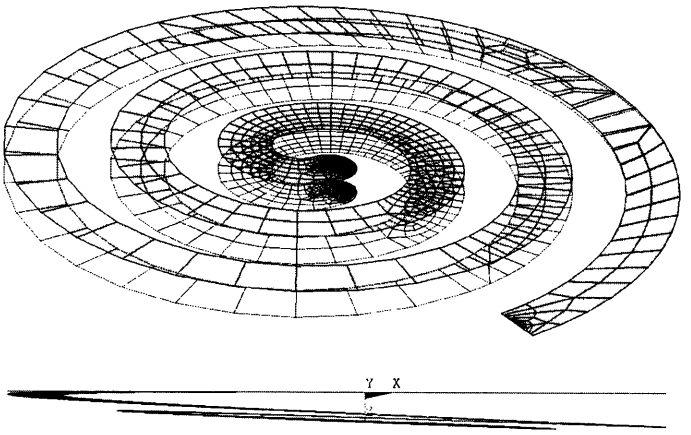

Figure 9: Primary mode of vibration.

of these higher frequency modes. This torsional motion is counterproductive for harvesting electrical energy from piezoelectric materials. The stress on one half of the total surface will be opposite the other half, leading to a cancellation of overall current. Uni-directional stress gives the maximum power from the beam.

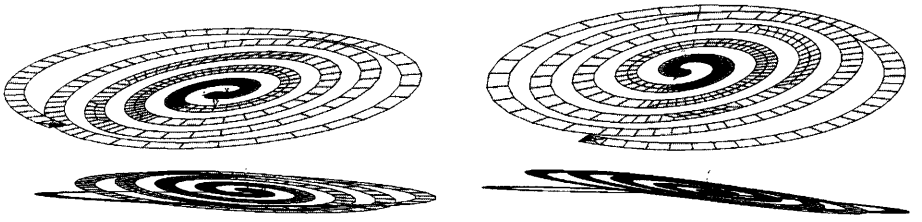

(a) 2nd Mode **(b)** 3rd Mode

Figure 10: Secondary and tertiary modes of vibration.

5 Experimental Methods

For the purpose of this project, a mock-up design of the PMPG is to be fabricated to further understand the relationship between shape and resonant frequency. This fabrication process is simplified from the process described in section 2.1. The polymer SU-8 was the beam's only material. [1]

5.1 Mock-Up Fabrication

In the same manner that the proof mass is constructed on the actual PMPG, a layer of SU-8 is first spin-coated onto the Silicon substrate. Spin-on is a commonly used process for dielectric insulators and organic materials. Simple equipment is all that is required. A liquid solution is sprayed onto the center of the wafer while the substrate spins on a table at speeds of up to 5000 rpm. The layer is spun to a thickness of 25 μm for all beam structures.

The SU-8 layer is then patterned using a mask designed for all the variations shown in Table 1. To separate the beam structures from the Silicon substrate, a standard SU-8 developer is used for etching. Finally, XeF_2 vapor etching was used to release the beam.

	Number of Turns=rad/(2π)				
	2.75	**3.25**	**3.75**	**4.25**	**4.75**
150 um	1	2	3	4	5
200 um	6	7	8	9	10
250 um	11	12	13	14	15

Table 1: A 3 x 5 matrix of beam variations of width and lengths. Listed are the beam identification numbers.

[1] At publication, the mock-up device was in the stages of fabrication and was incomplete. For this reason, only methods are presented here without experimental results.

5.2 Vibrometer Testing

A scanning laser vibrometer is used to test the dynamics of the beams [4]. The vibrometer has the ability to detect sub nanometer displacement. The laser beam is placed at the center of the device using the vibrometer's computer interface. Placing the beam at the center of the device, where any necessary proof masses would be added gives valuable information about the displacement at resonance of the beam structure. A piezoelectric shaker provides the input vibration to the PMPG.

The displacement data allows for a full spectrum of harmonic analysis. From this spectrum, the peaks of displacement represent the various natural frequencies and the primary mode can be determined. Damping and Q-factor can also be determined from this analysis.

The laser vibrometer system is also capable of scanning across the surface of the beam. From these scans digital video can be produced that shows exactly how the beam deflects at resonance. These images will allow for full verification of the ANSYS simulated mode shapes.

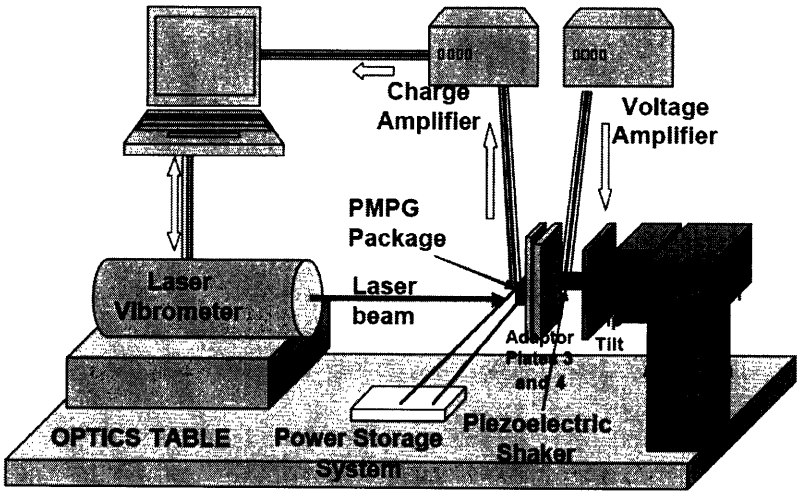

Figure 11: Schematic of the vibrometer setup. The charge amplifier is for gaining power information from actual PMPG devices and are not used for prototype testing here. [4]

6 Conclusions and Future Work

The relationship between spiral beam structures and their resonant frequencies has been characterized. Functions of their total length to their resonant frequencies were also related to those of one-dimensional cantilever beams. Several differences were observed. Spiral beams' natural frequencies have a dependence on width unlike their one-dimensional counterparts. They also exhibit higher resonant frequencies for equivalent lengths. These frequencies can be up to more than four times higher at the same lengths. It is observed that the resonant frequency of a spiral beam depends on length to a power of -1.3 rather than -2 as with regular beams. The first three mode shapes of spiral structures were also examined.

Finite element analysis is an essential tool for analyzing these complex structures' dynamic properties before fabrication. It gives more accurate results than any analytical methods this author has used. Further study on analytical methods may yield better results, but understanding the torsional and bending moments of the structure is complex.

To use spiral beam structures in PMPG devices, a method for estimation of damping and Q-factor should be further studied. Integrating that into this analysis of the spiral structure will give more accurate estimations of the primary resonant frequency and the power output.

Methods of properly promoting the primary mode of resonance while suppressing higher modes of resonance should also be developed. Controlling the direction of input vibration the beam feels is crucial to generating sufficient energy to make the PMPG a viable option for wireless sensing nodes. One suggestion may be to make several spiral structures, tethered in three-dimensions to a single proof mass. This decision will limit the effective degrees of freedom of the structure and attenuate some of the higher modes.

Structures of low resonant frequency are developed here which are also compact in size and shape suitable for packaging into a MEMS device [7]. A spiral beam is developed that, with 0.2% strain in the PZT layer, should produce near 1 μW of power. It has a width of 200 μm and is 3.25 turns in length. Damping will be a serious design concern in the future and is already being addressed in research.

References

[1] John DeGaspari. Pumped up: Micro-device manufacturers shift into high gear, as new federal rules give them millions of tires to ride. *Mechanical Engineering*, April 2005.

[2] Y. Jeon, R. Sood, L. Steyn, and S. G. Kim. Energy harvesting MEMS devices based on d_{33} mode piezoelectric $Pb(ZrTi)O_3$ thin film cantilever. In *Proceedings of Solid-State Sensor and Actuator Workshop*, volume 26. Hilton Head, SC, June 2004.

[3] S. Roundy, P.K. Wright, and J. Rabaey. A study of low level vibrations as a power source for wireless sensor nodes. *Computer Communications*, 26:1131–1144, 2003.

[4] Rajendra K. Sood. *Piezoelectric Micro Power Generator (PMPG): A MEMS Based Energy Scavenger.* Master's Thesis, Department of Computer Science and Electrical Engineering, Massachusetts Institute of Technology, Cambridge, MA, September 2003.

[5] C. F. Beards. *Structural Vibration: Analysis and Damping.* Halstead Press, New York, 1996.

[6] Daniel F. Opila. *Design of Free Cantilever Beams for the Piezoelectric Micro Power Generator (PMPG).* Bachelor's Thesis, Department of Mechanical Engineering, Massachusetts Institute of Technology, Cambridge, MA, June 2002.

[7] W. J. Choi, Y. Xia, J. A. Brewer, and S. G. Kim. Energy harvesting MEMS device based on thin film piezoelectric cantilevers. In *Proceedings of the Second International Workshop on Network Sensing Systems.* San Diego, CA, June 2005.

A ANSYS: Modal Analysis Code

```
/AUX15
    !IMPORT FILE
    IOPTN,IGES,NODEFEAT
    IOPTN,MERGE,YES
    IOPTN,SOLID,YES
    IOPTN,SMALL,YES
    IOPTN,GTOLER, DEFA
    IGESIN,'W150_L234','IGS',' '
    VPLOT
FINISH
/PREP7
    !PREPROCESSOR>ADD SHELL93
    ET,1,SHELL93
    !THICKNESSES DEFINED
    R,1,25E-3,25E-3,25E-3,25E-3, , ,
    R,2,25E-3,25E-3,25E-3,25E-3, , ,
    !MATERIAL MODEL 1 (BEAM) DEFINED
    MPTEMP,,,,,,,,
    MPTEMP,1,0
    MPDATA,EX,1,,.0402E8
    MPDATA,PRXY,1,,.22
    MPTEMP,,,,,,,,
    MPTEMP,1,0
    MPDATA,DENS,1,,2200E-9
    !MATERIAL MODEL 2 (PROOF MASS) DEFINED
    MPTEMP,,,,,,,,
    MPTEMP,1,0
    MPDATA,EX,2,,.0402E8
    MPDATA,PRXY,2,,.22
    MPTEMP,,,,,,,,
    MPTEMP,1,0
    MPDATA,DENS,2,,2200E-9
    !DRAW CIRCLE (PROOF MASS), OVERLAP, AND GLUE
    CYL4,0,0,5E-3
    ASEL,S,LOC,Z,0,0
    AOVLAP,ALL
    AGLUE,1,2
    !MESH THE BEAM
    MSHAPE,0,2D
    MSHKEY,0
    TYPE,   1
    MAT,       1
    REAL,       1
    ESYS,       0
```

```
    SECNUM,
    MSHKEY,0
    CM,_Y,AREA
    ASEL, , , ,       2
    CM,_Y1,AREA
    CHKMSH,'AREA'
    CMSEL,S,_Y
    AMESH,_Y1
    CMDELE,_Y
    CMDELE,_Y1
    CMDELE,_Y2
    !MESH THE PROOF MASS
    TYPE,   1
    MAT,       2
    REAL,       2
    ESYS,       0
    SECNUM,
    MSHKEY,0
    CM,_Y,AREA
    ASEL, , , ,       1
    CM,_Y1,AREA
    CHKMSH,'AREA'
    CMSEL,S,_Y
    AMESH,_Y1
    CMDELE,_Y
    CMDELE,_Y1
    CMDELE,_Y2
FINISH
/SOL
    !SELECT ANALYSIS TYPE/OPTIONS
    ANTYPE,2
    MSAVE,0
    MODOPT,LANB,10
    EQSLV,SPAR
    MXPAND,10, , ,0
    LUMPM,0
    PSTRES,0
    MODOPT,LANB,10,0,700, ,OFF
    !APPLY CONTRAINT TO FIXED END
    FLST,2,1,4,ORDE,1
    FITEM,2,192     !<--Line Number
    /GO
    DL,P51X, ,ALL,0
    !SOLVE
    /STATUS,SOLU
    SOLVE
FINISH
```